Journal of Rare Earths 36 (2018) 1106–1111

Contents lists available at ScienceDirect

Journal of Rare Earths

journal homepage: http://www.journals.elsevier.com/journal-of-rare-earths

Strongly correlated intermetallic rare-earth monoaurides (Ln-Au): *Ab-initio* study☆

Sardar Ahmad [a, b], M. Shafiq [b, d], Rashid Ahmad [a, b, *], S. Jalali-Asadabadi [c], Iftikhar Ahmad [b, d]

[a] Department of Chemistry, University of Malakand, Chakdara, Pakistan
[b] Center for Computational Materials Science, University of Malakand, Chakdara, Pakistan
[c] Department of Physics, Faculty of Sciences, University of Isfahan, Hezar Gerib Avenue, Isfahan 8174-73441, Iran
[d] Department of Physics, Abbottabad University of Science and Technology, Abbottabad, Pakistan

ARTICLE INFO

Article history:
Received 2 December 2017
Received in revised form
21 March 2018
Accepted 22 March 2018
Available online 29 May 2018

Keywords:
Strongly correlated electron systems
Rare-earth monoaurides
Mechanical properties
Ab-initio calculation

ABSTRACT

In this paper, we explored the structural, elastic and mechanical properties of the strongly correlated electron systems, intermetallic Ln-Au (Ln = Ce, Pr, Nd, Gd, Tb, Dy, Ho, Er, Tm, Yb, Lu) in cubic structure, using PF-LAPW method within the density functional theory. Structural properties of these intermetallics were investigated by treating the exchange-correlation potential with the GGA-PBE, GGA-PBEsol and GGA + U. The effectiveness of the U for the structural properties as compared to other methods confirms the strong correlated nature of these compounds and the calculated lattice constants endorse the divalency of Yb. The results demonstrate the stable cubic CsCl structure of these compounds. Bulk modulus, Young's modulus, shear modulus, *B*/*G* ratio, Cauchy pressure, Poisson's ratio, anisotropic ratio, Kleinman parameters and Lame's coefficients were studied using the PBEsol to evaluate their importance in various types of engineering applications. The most prominent features of these compounds are their ductility, very high melting points, resistance to corrosion, and anisotropic nature.

© 2018 Chinese Society of Rare Earths. Published by Elsevier B.V. All rights reserved.

1. Introduction

The strongly correlated electron systems, intermetallics Ln-Au (Ln = Ce, Pr, Nd, Gd, Tb, Dy, Ho, Er, Tm, Yb and Lu), exhibit the best combination of physical properties such as low density, high stiffness, high oxidation resistance, high strength, very high melting point, ductility, high corrosion resistance, high temperature mechanical properties, and electrical properties. These advantages make them promising candidates for high temperature structural materials for automobiles, aviation and aerospace applications, and also for the development of commercial aircraft turbines.[1–3] These rare-earth monoaurides intermetallics (Ln-Au), are very attractive compounds for chemists, physicists and engineers because of their extensive high-tech applications.[4]

Binary alloys of gold with rare earths are normally characterized by the cubic CsCl-type crystal structure (*B*2, *Pm*3*m*, space group No. 221)[5–7] with the exception of CeAu[6] with CrB-type crystal structure.[1,8] Although, experiments also show cubic CsCl-type structure for CeAu.[9] In CsCl-type structure, Ln atoms are at the corners and Au atom is located at the body centered position of the cubic unit cell.[9] Lanthanides in these compounds exist in trivalent state[1,10,11] except Yb that is present in divalent state.[12–14] The divalent nature is established from its unusual high lattice constant compared to other members of the series. Generally these compounds exist in anti-ferromagnetic nature.[15]

Lanthanides make the first group of compounds containing f-orbitals,[16,17] where compounds with f-orbitals react differently than the other groups of the periodic table.[18] One of its fascinating subgroup is compounds of lanthanides with noble metals based stable lanthanides. The most stable among these unique intermetallics are compounds containing gold because of their very high dissociation energies. Their dissociation energies are in the range of 290–335 kJ/mol with some irregularities.[1,19] The order of their bond stabilities is Au-Ln > Cu-Ln > Ag-Ln.[2]

The Ln-Au are synthesized by various researchers using direct reaction at high temperature (~1373 K). In their research, the reactants in powder form were sealed under argon atmosphere in a

☆ **Foundation item:** Project supported by the Higher Education Commission of Pakistan (HEC) (20-3959/NRPU/R&D/HEC2014/119).
* Corresponding author. University of Malakand, Chakdara, Pakistan.
E-mail address: rashmad@gmail.com (R. Ahmad).

https://doi.org/10.1016/j.jre.2018.03.018
1002-0721/© 2018 Chinese Society of Rare Earths. Published by Elsevier B.V. All rights reserved.

boron nitride container to prevent oxidation.[20] The reaction is highly exothermic and the evolved heat in the range of $\Delta H_f^0 = -63.0$ to −95.0 kJ/mol, is used for completion of the reaction.[21,22] Thus stable compounds are formed.[20] The X-ray diffraction data confirm the cubic CsCl type structure for these compounds.[20,23] The heat of formation of these compounds decreases and melting point increases along the series from CeAu to LuAu.[19] Their very high melting points, ionic nature and high dissociation energies are due to the big electronegativity difference i.e. >1.13 and equiatomic stoichiometry of lanthanides and gold.[2,10,24] The anomalously high thermal stability of these compounds is due to their high heat of formation and high melting points.[19,24,25] A correlation exists between their stability trend and relative melting behaviors.[22] The melting points of these aurides increase in a smooth fashion as a function of atomic number of lanthanides from CeAu (1372 °C) to LuAu (1780 °C) with the exception of YbAu (1292 °C).[7] The lower melting point of YbAu is due to the divalency of Yb.[26] Rare-earth addition to gold enhances the strength of gold alloys.[3] The gold and rare-earth elements form compounds because of their greater electronegativity difference. Therefore, bond between Au and R is metallic and ionic in nature, where metallic and ionic characters are 95% and 5%, respectively.[1,19,22] However, Dayán Páez-Hernández et al.[27] recently determined the bond nature of rare earth-gold (Ln-Au_2) molecules (Ln = Eu, Yb and Lu) using CASSCF/CASPT2 calculations and predicted a greater covalent character with important contribution from bonding interaction between the 6s orbital of Au and 6s orbital of Ln atoms. This can be inferred from their high melting points, high dissociation energies, thermal stability and bond energies.[21] Their bond energies are from 3.3 to 3.4 eV.[28]

Although these compounds are very important due to their high-tech applications, but even then limited experimental and theoretical studies have been reported about them. To the best of our knowledge no experimental or theoretical work on the elastic and mechanical properties of these compounds is reported in literature, however limited theoretical and experimental work is available on their structural properties. In this manuscript we have carried out detailed theoretical studies of the structural, elastic and mechanical properties of these rare-earth monoaurides, Ln-Au (Ln = Ce, Pr, Nd, Gd, Tb, Dy, Ho, Er, Tm, Yb, Lu), with the realization to cover the gap of the physical properties of these compounds in literature and reveal their potential applications in various technologies.

2. Computational details

The complete active space self-consistent field (CASSCF)[29] and multiconfigurational second-order perturbation method CASPT2[30] are the valuable tools in chemical physics and theoretical chemistry to compute properties such as dissociation energies, geometry parameters, and chemical bonds. CASSCF and CASPT2 approaches play an important role in the development of a molecular understanding of structures and processes. These approaches constitute the appropriate starting point for wave function descriptions of small molecules and complexes containing transition metals.[31] However, quite often these methods are associated with calculations of very small molecules. The choice of computational method depends on the properties and the kind of systems under study. Some systems like solids, aggregates, complexes require size extensive methods. DFT gained much attention over wave function theory in order to describe the electronic states of atoms, molecules and materials in terms of the electronic density of the system. This is due to the fact that cost scales more favorably with system size than does the cost of correlated wave function theory and yet it competes well in accuracy except for very small systems.[32]

Due to electrons correlation and other relativistic effects, the computational calculations of large systems and heavy elements (rare-earths) are very difficult. One must treat these systems by including inactive core electrons and relativistic effects, which required very expensive calculations. Quantum chemical calculations for large systems including heavy elements are difficult to carry out because of electron correlation and other relativistic effects. In the standard all-electron theory, one must treat many electrons including inactive core electrons in heavy elements. One must also simultaneously treat relativistic effects, resulting in high-cost calculations. Performing calculations on in active space method such as CASSCF and CASPT2 required more knowledge about the system under investigation, properties being calculated than other quantum chemistry method such as DFT. Different active space is used for calculating different properties of a system. Furthermore, the knowledge of orbitals composing the wave function is very important for the molecular properties of a system under study. However, DFT is simple and commonly used as black box quantum chemistry method. Due to this fact we used DFT instead of other sophisticated method in the present work for our calculations.

In this work, we performed spin polarized calculations using the full-potential linearized augmented plane waves (FP-LAPW) method based on the density functional theory (DFT) employing the exchange-correlation potentials of the generalized gradient approximation (GGA) with two different parameterizations i.e. PBE and PBEsol[33–36] as well as GGA with Hubbard U potential (GGA + U) as implemented in the wien2k code.[37–39] The number of *k*-points was optimized and all the calculations are performed at 1000 *k*-points. The brillouin-zone integration was performed using maximum value of angular momentum $l_{max} = 10$. The muffin-tin radii (R_{MT}) for lanthanide atoms (Ln) and Au atom are considered as 2.5 a.u., while the charge density is Fourier expanded up to $G_{max} = 12.00$ Ry.

The Cubic-elastic software[40,41] and PBE-sol exchange correlation were utilized to calculate the elastic and mechanical properties of the compounds under study. To obtain the reliable results we used the energy approach[42] implemented in WIEN2k package. The energy that separates the valence states from the core states has been considered as −6.0 Ry. The convergence parameter, $R_{MT}K_{max}$, which controls the size of the basis set in these calculations, is set at 7.5, where R_{MT} is the smallest atomic radius in the unit cell while K_{max} is the magnitude of the maximum value of k-vector in the plane wave expansion.

3. Results and discussion

3.1. Structural properties

Structural properties of Ln-Au (Ln = Ce, Pr, Nd, Gd, Tb, Dy, Ho, Er, Tm, Yb, Lu) intermetallics were calculated by evaluating the optimized total energy of unit cell for each compound with respect to volume using Birch-Murnaghan equation of state.[43] The lattice constants of all compounds are obtained by GGA-PBEsol, GGA-PBE and GGA with Hubbard U exchange correlation potentials. The calculated results are compared with the available experimental data in Table 1. It is obvious from the data presented in Table 1 and Fig. 1 that PBE overestimates and PBEsol underestimates the lattice constants of the compounds under study. For strongly correlated systems the application of U is effective for the localization of electrons and hence we obtained closer values for the lattice constants. Table 1 shows that as we move from CeAu to LuAu, the lattice constant of the crystal decreases. This decrease is due to the lanthanide contraction, i.e. decrease in the atomic radius along the lanthanide series from left to right. The lanthanide contraction is

Table 1
Calculated lattice constants ($\times 10^{-1}$ nm) by PBEsol, PBE and U compared with the experimental and reported theoretical results.

Compound	PBEsol	PBE	Reported	U	Expt.
CeAu	3.66	3.75	3.59[b]	3.6777	3.70[b]
PrAu	3.68	3.69	3.75[b]	3.6868	3.68[a]
NdAu	3.62	3.70	3.72[b]	3.6984	3.66[a]
GdAu	3.57	3.64	3.63[b]	3.625	3.59[c]
TbAu	3.55	3.62	3.62[b]	3.611	3.58[a]
DyAu	3.55	3.59	3.56[b]	3.5862	3.56[a]
HoAu	3.53	3.59	3.58[b]	3.551	3.54[a]
ErAu	3.51	3.59	3.57[b]	3.5674	3.53[a]
TmAu	3.50	3.54	–	3.5459	3.52[c]
YbAu	5.53	3.59	–	3.5831	3.58[a]
LuAu	3.47	3.52	3.53[d]	3.5173	3.49[c]

[a] Ref. 7.
[b] Ref. 9.
[c] Ref. 6.
[d] Ref. 65.

caused by the poor shielding effect of the 4f electrons, with the exception of Eu and Yb.

The theoretical calculations and experimental results presented in Fig. 1 clearly reveal the unusual increase in the lattice parameter of YbAu. This unique behavior of the Yb is because of its divalent nature as compared to other trivalent lanthanides. The divalent nature of Yb is due to the attainment of completely filled configuration of $4f^{14}$ by losing $6s^2$ electrons. The completely filled electronic configuration is more stable than partially filled electronic configuration. In divalent state charge is smaller. Therefore, the force of attraction is smaller which results in low melting point, smaller cohesive energy and least ionic character of YbAu.[26] Fig. 1 also shows comparison between different theoretical calculations with the experimental measurements. It is clear from the figure that PBE and PBEsol shows overestimation and underestimation respectively for the lattice constant of all the compounds. Table 1 clearly reveals that for most of the compounds under consideration the PBEsol provides much more reasonable theoretical results, closer to the experimental values, as compared to the reported theoretical results,[6,7] as well as PBE calculations.

3.2. Elastic and mechanical properties

The elastic properties of a substance explain that how a material undergoes stress deformation and recovers its original shape after stress is released. These properties play an important role in providing valuable data about the mechanical properties of a material such as type of bonding, structural stability, hardness, and ductility, etc.[44] Elastic properties are also linked with the thermodynamic properties of materials like specific heat, Debye temperature, Gruneisen parameter and thermal expansion. Therefore, the knowledge of the elastic constants for materials especially engineering materials is necessary for their practical applications related to their structure stability and other physical properties such as internal strain, thermoelastic stress, sound velocities, fracture toughness and Debye temperature, etc.[33,45,46] There are three independent elastic constants for cubic crystal i.e. C_{11}, C_{12} and C_{44}.[40,47,48] The stability of cubic structure can easily be inferred by the well-known Born criteria ($C_{11}-C_{12} > 0$, $C_{44} > 0$, $C_{11} + 2C_{12} > 0$).[49,50] The elastic constants of the compounds under study were calculated by PBEsol and presented in Table 2.

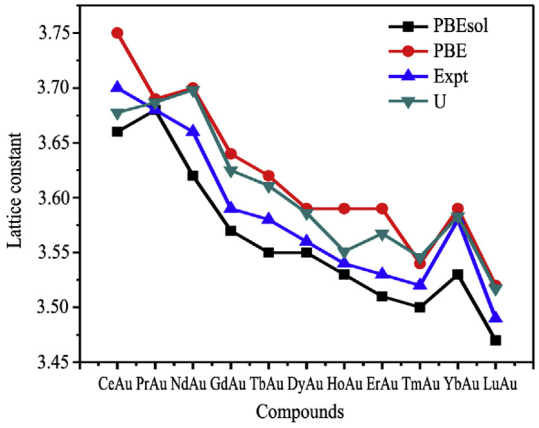

Fig. 1. Comparison of the calculated lattice constants of Ln-Au by PBEsol, PBE and Hubbard U with the experimental values.

The elastic constants given in Table 2 were used to evaluate the mechanical properties, i.e. Bulk modulus (B_0), Shear modulus (G), Young's modulus (Y), Poisson's ratio (ν) and anisotropic ratio (A), of the compounds under study. These properties have vital importance for the industrial applications of engineering materials.[51,52] These important parameters for these compounds were calculated using PBEsol to evaluate their possible high-tech engineering applications and presented in Table 2.

One of the utmost important parameters of the high-tech materials is bulk modulus. The bulk modulus (B_0) of a material is the measure of its hardness. It can be computed from the elastic constants using the following relation:

$$B_0 = \frac{C_{11} + 2C_{12}}{3} \quad (1)$$

It can also be used to measure the average bond strength since it has a strong correlation with the cohesive or binding energy of atoms in a crystal.[53] The calculated values of the bulk moduli for the compounds under study are given in Table 2. This clearly indicates that the bonding nature of these compounds is ionic/metallic. Average Shear modulus (G_H) is the measure of plastic deformations upon shear stress which is an important mechanical property.[33,54] The shear modulus G accurately determines the hardness of a material. As per Hill average shear modulus,[54] G is defined as the arithmetic mean of Voigt (G_V)[40] and Reuss (G_R) values, which can be expressed in terms of elastic constants as:

$$G_V = \frac{1}{5}(3C_{44} + C_{11} - C_{12}) \quad (2)$$

$$G_R = \frac{5(C_{11} - C_{12})C_{44}}{4C_{44} + 3(C_{11} - C_{12})} \quad (3)$$

$$G_H = \frac{G_V + G_R}{2} \quad (4)$$

The calculated values of G_H using the above relation are provided in Table 2, which reveal that LuAu exhibits the largest value of G_H (36.046 GPa) being the hardest of all the compounds, while DyAu shows less hardness with the lowest value of G_H (21.488 GPa). This fact is supported by their melting points. Values of G_H for the remaining compounds lie between these two values.

Another similar mechanical property that measures the stiffness of an elastic material is called Young's modulus (Y). Greater value of Y corresponds to stiffness of a material. The Young's modulus for these compounds were calculated by using the values of Voigt shear modulus (G_V) and bulk modulus (B_0) in the following relation:

$$Y = \frac{9B_0G_V}{3B_0 + G_V} \quad (5)$$

Table 2
Calculated values of elastic constants C_{11}, C_{12}, C_{44} (GPa), Bulk modulus B_0 (GPa), Voigt's shear modulus G_V, Reuss shear modulus G_R, Hill's shear modulus G_H, Young's modulus Y (GPa), B/G ratio, Cauchy pressure C'', Poission ratio ν, Internal strain parameter ξ, anisotropy A, Lamé's first parameter λ, Lamé's second parameter μ and Shear constant C'.

Compound	CeAu	PrAu	NdAu	GdAu	TbAu	DyAu	HoAu	ErAu	TmAu	YbAu	LuAu
C_{11}	98.078	89.408	84.700	87.852	83.500	84.451	83.936	81.732	91.207	89.901	107.596
C_{12}	55.798	35.916	39.500	45.921	34.751	41.445	39.902	39.366	51.758	29.418	44.436
C_{44}	27.519	22.219	23.400	27.453	21.281	21.479	24.834	31.024	30.800	23.578	39.374
B_0	69.80	53.747	54.567	59.898	51.001	55.780	54.580	53.488	64.908	49.579	65.489
G_v	24.967	24.030	23.080	24.858	22.518	21.489	23.707	27.088	26.370	26.243	36.256
G_R	24.555	23.833	23.073	24.429	22.419	21.489	23.625	26.162	25.151	25.857	35.836
G_H	24.761	23.931	23.077	24.644	22.469	21.489	23.666	26.625	25.760	26.050	36.046
Y	66.92	62.739	60.684	65.511	58.888	57.130	62.127	69.526	69.674	66.922	91.824
B/G	2.820	2.246	2.365	2.431	2.270	2.596	2.306	2.009	2.520	1.903	1.817
C''	28.279	13.697	16.100	18.468	13.470	19.966	15.068	8.342	20.958	5.840	5.062
ν	0.34	0.305	0.315	0.318	0.308	0.329	0.310	0.283	0.321	0.275	0.266
ξ	0.947	0.680	0.780	0.870	0.702	0.818	0.165	0.804	0.945	0.570	0.697
A	1.302	0.831	1.035	1.309	0.873	0.999	1.128	1.465	1.562	0.780	1.247
λ	53.16	37.727	39.180	43.326	35.988	41.455	38.775	35.430	47.328	32.083	41.318
μ	24.967	24.030	23.080	24.858	22.518	21.489	23.707	27.088	26.370	26.243	36.256
C'	21.140	26.746	22.600	20.966	24.375	21.503	22.017	21.183	19.725	30.242	31.580

The values of Bulk modulus, Young's modulus and Shear modulus are given in Table 2. The intermediate values of Y of these compounds show that these materials are intermediate in stiffness.[46] It is evident from Table 2 that the materials under investigation have higher values of Young's modulus in comparison with Bulk moduli and Shear moduli; hence these compounds are hard to break.

The Pugh's ratio (B_0/G) is an essential parameter that explains the ductile/brittle nature of materials. The material is considered ductile if this ratio is larger than 1.75, otherwise it is brittle.[23,51,55] The B_0/G ratio for the compounds under study is given in Table 2 which confirms that these values are larger than 1.75. Therefore, all the compounds are ductile in character. Among these compounds the highest B_0/G ratio is observed for CeAu which is 2.82, indicating its highest ductility. Another important parameter is Cauchy pressure, used to illustrate the bonding nature of compounds.[23,56] This parameter can be calculated by using the relation:

$$C'' = C_{12} - C_{44} \tag{6}$$

The calculated values of the Cauchy pressures are presented in Table 2. The positive value of Cauchy pressure reveals ionic[33,47,57] and metallic[23,53,56] nature of bonding, while its negative value indicates covalent bonding. In addition, a compound with larger negative value of Cauchy pressure shows stronger brittle behavior.[58] Table 2 clearly indicates that the compounds under consideration have positive values of Cauchy pressure and are ionic/metallic and ductile in nature. The most ionic/metallic compound among these compounds is CeAu and the least ionic/metallic compound is LuAu.

Poisson's ratio (ν) is a response of the materials to different amounts of stress and provides a way to differentiate the structural performance of real materials. It is defined as the ratio of transverse strain to longitudinal strain in uniaxial tensile stress. The compound will be incompressible when Poisson's ratio is 0.5 and will be compressible if it is 0.2 to 0.49.[59] The Poisson's ratio for a material can be calculated by using the values of Young's modulus and Bulk modulus in the following relation:

$$\nu = \frac{1}{2} - \frac{Y}{6B_0} \tag{7}$$

The calculated values of the Poisson's ratio of Ln-Au's are provided in Table 2. For most metallic materials ratio lies between 0.25 and 0.35. The Poisson's ratio for Ln-Au varies between 0.266 and 0.34, confirming the intermetallic nature of these compounds. Poisson's ratio also provides information about the bonding forces.[46] For central forces in solids materials, the lower and upper limit of Poisson's ratio is 0.25 and 0.50, respectively.[46] The calculated values of Poisson's ratio ranging from 0.266 to 0.34 fall within the above mentioned limit, which demonstrates that central atomic forces are dominated in these compounds.

The anisotropic ratio (A) is the measure of intensity of a property in different directions. When A is equal to unity the material will be isotropic otherwise anisotropic. The elastic anisotropy (A) is highly correlated with the possibility of the induced micro cracks in a material and has vital importance in engineering materials for their applications.[46,60] The anisotropic ratio for a material from the elastic constants can be obtained by the following equation:

$$A = \frac{2C_{44}}{C_{11} - C_{12}} \tag{8}$$

The calculated anisotropic values in Table 2 reveal that the anisotropic ratio for most of the Ln-Au compounds deviate from one. The deviation from unity confirms that all these compounds are elastically anisotropic except NdAu and DyAu. The anisotropic ratio for NdAu and DyAu compounds is almost unity, which demonstrates the isotropic behavior of these materials. These two compounds also satisfy the other conditions for isotropy that is $\lambda = C_{12}$, $\mu = C_{44}$, and ν must be $-1 \leq \nu \leq ½$.[61]

Kleinman[62] presented an important mechanical property called internal strain parameter (ζ), that describes the relative case of bond bending to bond stretching. Its value lies between 0 and 1, where 0 shows minimum bond bending or bond angle distortion, and 1 shows minimum bond stretching.[47] The Kleinman parameter is given by the following mathematical expression:

$$\zeta = \frac{C_{11} + 8C_{12}}{7C_{11} - 2C_{12}} \tag{9}$$

The computed values of the Kleinman parameters for PrAu, NdAu, GdAu, HoAu, ErAu, YbAu, TmAu, YbAu, and LuAu lie between 0.5 and 0.9 and hence bond bending is dominated in these compounds. The very small value for HoAu shows the dominated bond stretching.

One more mechanical property that controls the isotropic nature of a material is called Lame's constants (λ, μ). Any material is isotropic when $\lambda = C_{12}$ and $\mu = C'$. Lame's constants can be calculated by using the following equations,

$$\lambda = \frac{Y\nu}{(1+\nu)(1-2\nu)} \text{ and } \mu = \frac{Y}{2(1+\nu)} \quad (10)$$

The equation shows that higher value of Young's modulus corresponds to the larger values of Lame's coefficients. The calculated values of the Lame's coefficients for Ln-Au compounds are given in Table 2. It is clear from the table that only NdAu and DyAu are isotropic in nature which is consistent with our previous results. Shear modulus (C') also known as tetragonal shear modulus that describes the dynamical stability of a compounds can be calculated as:

$$C' = \frac{1}{2}(C_{11} - C_{12}) \quad (11)$$

The criterion for dynamical stability of a compound needs $C' > 0$, while the negative value of C' indicates the instabilities of a compound with respect to the tetragonal distortion as reported in experimental work.[63] The calculated values for the shear constants of Ln-Au compounds are listed in Table 2. The positive values ($C' > 0$) of the Ln-Au compounds predict that these are mechanically stable materials.

3.3. Thermodynamic properties

Debye temperature is an important parameter, related to many physical properties such as specific heat, elastic constants and melting point. It also corresponds to the lattice vibrations in a crystal. Debye temperature is directly proportional to average sound velocity and can be calculated by using the following relationship.[64]

$$\Phi(D) = \frac{h}{k_B}\left[\frac{3n}{4\pi}\left(\frac{N_A\rho}{M}\right)\right]^{\frac{1}{3}}\nu_m \quad (12)$$

where h is plank constant, k_B Boltzmann constant, N_A Avogadro's number, M the molecular weight, ν_m the average sound velocity, n the number of atoms in the molecule and ρ the theoretical density which can be calculated as

$$\rho = \frac{n \times M}{\nu_c \times N_A} \quad (13)$$

where n is the number of atoms per formula unit. For CsCl crystal structure, $n = 1$, M is the molecular mass of the compound, ν_c the unit cell volume and N_A the Avogadro's number.

The average sound velocity, ν_m can be obtained as[33]:

$$\nu_m = \frac{1}{3}\left[\frac{2}{{\nu_s}^3} + \frac{1}{{\nu_l}^3}\right]^{-\frac{1}{3}} \quad (14)$$

where ν_l and ν_s are the longitudinal and transverse sound velocities, which can be obtained using the shear modulus G and the Bulk modulus B_0 from Navier's equations[44]:

$$\nu_l = \left[\frac{B + 4\frac{G}{3}}{\rho}\right]^{\frac{1}{2}} \text{ and } \nu_s = \left[\frac{G}{\rho}\right]^{\frac{1}{2}} \quad (15)$$

The calculated values of sound velocity, for longitudinal and shear waves (ν_l and ν_s), and average sound velocity (ν_m) and Debye temperature for Ln-Au compounds are presented in Table 3. As all these materials are anisotropic, the sound velocities in these materials strongly depend on the direction of propagation. It is clear from Table 3 that the LuAu exhibits higher value of Debye temperature than the remaining compounds, hence LuAu is more stiffer than other compounds, confirming the results of Young's modulus (LuAu, $Y = 91.824$). The lower and higher values of sound velocities and Debye temperature are the consequences of higher and lower elastic moduli.

Table 3
Calculated values of density (ρ), sound velocity of transverse, longitudinal and average sound velocity (ν_s, ν_l and ν_m), and Debye temperature ($\theta(D)$) of Ln-Au compounds.

Comp.	ρ (g/cm^3)	ν_l (m/s)	ν_s (m/s)	ν_m (m/s)	$\theta(D)$ (K)
CeAu	11.049	2953.41	1340.91	1511.74	121.65
PrAu	11.258	2812.53	1325.47	1491.70	120.70
NdAu	11.566	2716.25	1412.51	1580.71	128.63
GdAu	12.596	2601.77	1229.00	1382.97	114.35
TbAu	12.924	2502.85	1318.53	1474.26	122.76
DyAu	13.286	2520.86	1271.74	1425.90	119.43
HoAu	13.536	2618.54	1246.74	1402.37	117.92
ErAu	13.691	2536.96	1375.61	1534.93	129.29
TmAu	13.930	2643.85	1322.92	1484.00	125.53
YbAu	13.346	2513.43	1397.09	1555.95	129.27
LuAu	14.455	2504.73	1503.70	1663.36	141.67

4. Conclusions

In conclusion, we investigated structural, elastic and mechanical properties of Ln-Au (R = Ce, Pr, Nd, Gd, Tb, Dy, Ho, Er, Tm, Yb and Lu) intermetallics computationally with PBEsol and PBE exchange correlation potentials within the framework of density functional theory. It is deduced that these compounds are strongly correlated, because lattice constant calculated with Hubbard U are more accurate than calculated with other potentials. They are elastically stable, because they obey Born stability criteria. These compounds are hard and their melting points are very high which can be inferred from their high bulk and shear's moduli. The values of Young's moduli of these compounds indicate their intermediate stiffness, however, the positive values of their Cauchy pressure reveal that the bonding nature is predominantly metallic/ionic. Furthermore, the large values of the B_0/G ratio of these compounds show their ductile nature and the most ductile is CeAu with the highest B_0/G value of 2.82. The Poisson's ratio demonstrates that these compounds are less compressible and the deviation from unity of the isotropic ratio reveals that they are anisotropic except DyAu and NdAu. Furthermore, the internal strain parameter confirms bond bending for all the compounds except HoAu which shows bond stretching. These promising mechanical properties verify that these high temperature structural materials can be efficiently used in automobiles, aviation, and aerospace applications.

Acknowledgements

The authors acknowledge financial support from Higher Education Commission of Pakistan (HEC), Project No. 20-3959/NRPU/R&D/HEC2014/119. The authors are also thankful of Center for Computational Materials Science, University of Malakand, Pakistan for computing and technical supports.

References

1. Ning YT. Alloying and strengthening of gold via rare earth metal additions. *Gold Bull.* 2001;34(3):77.
2. Schwerdtfeger P, Dolg M. Anomalous high gold-metal bond stabilities: relativistic configuration-interaction calculations for AuLa and AuLu. *Phys Rev A.* 1991;43(3):1644.
3. Ning YT. Properties and applications of some gold alloys modified by rare earth additions. *Gold Bull.* 2005;38(1):3.

4. Wang MJ, Mu SM, Sun FF, Wang Y. Influence of rare earth elements on microstructure and mechanical properties of cast high-speed steel rolls. *J Rare Earths*. 2007;25(4):490.
5. Saccone A, Macciò D, Delfino S, Ferro R. The neodymium-gold phase diagram. *Metall Mater Trans A*. 1999;30(5):1169.
6. Chao CC. In: California Institute of Technology, ed. *A study of CsCl type intermediate phases involving rare earth elements*. 1965.
7. McMasters O, Gschneidner Jr K, Bruzzone G, Palenzona A. Stoichiometry, crystal structures and some melting points of the lanthanide-gold alloys. *J Less Common Met*. 1971;25(2):135.
8. Ferro R, Saccone A, Maccio D, Delfino S. A survey of gold intermetallic chemistry. *Gold Bull*. 2003;36(2):39.
9. Wu YR, Hu WY, Han SC. Theoretical calculation of thermodynamic data for gold-rare earth alloys with the embedded-atom method. *J Alloys Compd*. 2006;420(1):83.
10. Saccone A, Macciò D, Delfino S, Ferro R. Alloying behavior of the rare earth metals with gold: the Ho–Au, Er–Au and Tm–Au systems. *Intermetallics*. 2002;10(9):903.
11. Zhou XM, Li QB. Solid solubility metastable extension of rare earth metals in gold. *Gold Bull*. 1997;30(2):63.
12. Iandelli A, Palenzona A. The ytterbium-gold system. *J Less Common Met*. 1969;18(3):221.
13. Asadabadi SJ, Akbarzadeh H. Density functional approach to study structural properties and electric field gradients in rare earth materials. *Phys B Condens Matter*. 2004;349(1):76.
14. Asadabadi SJ, Cottenier S, Akbarzadeh H, Saki R, Rots M. Valency of rare earths in RIn_3 and RSn_3: *Ab initio* analysis of electric-field gradients. *Phys Rev B*. 2002;66(19):195103.
15. Kissell F, Wallace W. Magnetic characteristics of some 1: 1 compounds of the lanthanides with gold and aluminum. *J Less Common Met*. 1966;11(6):417.
16. Xue DF, Su CT, Chen XY. Hybridized valence electrons of $4f^{0-14}5d^{0-1}6s^2$: the chemical bonding nature of rare earth elements. *J Rare Earths*. 2017;35(8):837.
17. Sadri F, Nazari AM, Ghahreman A. A review on the cracking, baking and leaching processes of rare earth element concentrates. *J Rare Earths*. 2017;35(8):739.
18. Kurzen H, Bovigny L, Bulloni C, Daul C. Electronic structure and magnetic properties of lanthanide 3+ cations. *Chem Phys Lett*. 2013;574:129.
19. Gingerich K. Stability of rare-earth-containing high-temperature molecules. *J Less Common Met*. 1985;110(1):41.
20. Meschel S, Kleppa O. Thermochemistry of some binary alloys of gold with the lanthanide metals by high temperature direct synthesis calorimetry. *J Alloys Compd*. 2004;363(1):242.
21. Chao C, Luo H, Duwez P. CsCl-type compounds in binary alloys of rare-earth metals with gold and silver. *J Appl Phys*. 1963;34(7):1971.
22. Borzone G, Raggio R, Ferro R. Thermochemistry and reactivity of rare earth metals. *Phys Chem Chem Phys*. 1999;1(7):1487.
23. Zhao LR, Chen K, Yang Q, Rodgers JR, Chiou SH. Materials informatics for the design of novel coatings. *Surf Coating Technol*. 2005;200(5):1595.
24. Gingerich K, Finkbeiner H. Mass spectrometric determination of the dissociation energies of LaAu, CeAu, PrAu, and NdAu and predicted stability of gaseous monoaurides of electropositive metals. *J Chem Phys*. 1970;52(6):2956.
25. Ferro R, Borzone G, Parodi N. Comments on the formation thermodynamics of selected groups of rare earth compounds. *J Alloys Compd*. 2001;321(2):248.
26. Brewer L. Energies of the electronic configurations of the lanthanide and actinide neutral atoms. *JOSA*. 1971;61(8):1101.
27. Páez-Hernández D, Muñoz-Castro A, Arratia-Perez R. Bonding in gold-rare earth $[Au_2M](M{=}Eu, Yb, Lu)$ ions. A strong covalent gold-lanthanide bond. *Chem Phys Lett*. 2017;683:421.
28. Gingerich K, Finkbeiner H. Experimental and predicted bond energies of gaseous rare-earth aurides. *J Chem Soc D Chem Commun*. 1969;16:901.
29. Roos BO, Taylor PR, Si PE. A complete active space SCF method (CASSCF) using a density matrix formulated super-CI approach. *Chem Phys*. 1980;48(2):157.
30. Andersson K, Malmqvist PÅ, Roos BO. Second-order perturbation theory with a complete active space self-consistent field reference function. *J Chem Phys*. 1992;96(2):1218.
31. Olsen J. The CASSCF method: a perspective and commentary. *Int J Quant Chem*. 2011;111(13):3267.
32. Cramer CJ, Truhlar DG. Density functional theory for transition metals and transition metal chemistry. *Phys Chem Chem Phys*. 2009;11(46):10757.
33. Shafiq M, Arif S, Ahmad I, Asadabadi SJ, Maqbool M, Aliabad HR. Elastic and mechanical properties of lanthanide monoxides. *J Alloys Compd*. 2015;618:292.
34. Ahmad S, Ahmad R, Bilal M, Rehman NU. DFT studies of thermoelectric properties of R-Au intermetallics at 300K temperature. *J Rare Earths*. 2018;36:197.
35. Ahmad S, Vaizie H, Rahnamaye Aliabad H, Ahmad R, Khan I, Ali Z, et al. First-principles studies of pure and fluorine substituted alanines. *Int J Mod Phys B*. 2016;30(14):1650079.
36. El Hachimi A, Zaari H, Benyoussef A, El Yadari M, El Kenz A. First-principles prediction of the magnetism of 4f rare-earth-metal-doped wurtzite zinc oxide. *J Rare Earths*. 2014;32(8):715.
37. Galli G. Linear scaling methods for electronic structure calculations and quantum molecular dynamics simulations. *Curr Opin Solid State Mater Sci*. 1996;1(6):864.
38. Ahmad S, Ahmad R, Jalali-Asadabadi S, Ali Z, Ahmad I. First principle studies of electronic and magnetic properties of Lanthanide-Gold (RAu) binary intermetallics. *J Magn Magn Mater*. 2017;422:458.
39. Bian L, Song MX, Zhou TL, Zhao XY, Dui QQ. Band gap calculation and photo catalytic activity of rare earths doped rutile TiO_2. *J Rare Earths*. 2009;27(3):461.
40. Jamal M, Asadabadi SJ, Ahmad I, Aliabad HR. Elastic constants of cubic crystals. *Comput Mater Sci*. 2014;95:592.
41. Shafiq M, Ahmad I, Asadabadi SJ. Theoretical studies of strongly correlated rare-earth intermetallics RIn_3 and RSn_3 (R= Sm, Eu, and Gd). *J Appl Phys*. 2014;116(10):103905.
42. Stadler R, Wolf W, Podloucky R, Kresse G, Furthmüller J, Hafner J. Ab initio calculations of the cohesive, elastic, and dynamical properties of $CoSi_2$ by pseudopotential and all-electron techniques. *Phys Rev B*. 1996;54(3):1729.
43. Birch F. Finite strain isotherm and velocities for single-crystal and polycrystalline NaCl at high pressures and 300° K. *J Geophys Res Solid Earth (1978–2012)*. 1978;83(B3):1257.
44. Badehian HA, Salehi H, Ghoohestani M. First-principles study of elastic, structural, electronic, thermodynamical, and optical properties of yttria (Y_2O_3) ceramic in cubic phase. *J Am Ceram Soc*. 2013;96(6):1832.
45. Bouhemadou A, Khenata R, Kharoubi M, Seddik T, Reshak AH, Al-Douri Y. FP-APW+ lo calculations of the elastic properties in zinc-blende III-P compounds under pressure effects. *Comput Mater Sci*. 2009;45(2):474.
46. Yuan PF, Ding ZJ. *Ab initio* calculation of elastic properties of rock-salt and zinc-blend MgS under pressure. *Phys B Condens Matter*. 2008;403(12):1996.
47. Bilal M, Shafiq M, Ahmad I, Khan I. First principle studies of structural, elastic, electronic and optical properties of Zn-chalcogenides under pressure. *J Semiconduct*. 2014;35(7):072001.
48. Kalarasse F, Kalarasse L, Bennecer B, Mellouki A. Elastic and electronic properties of Li_2ZnGe. *Comput Mater Sci*. 2010;47(4):869.
49. Karki B, Ackland G, Crain J. Elastic instabilities in crystals from *ab initio* stress-strain relations. *J Phys Condens Matter*. 1997;9(41):8579.
50. Mouhat F, Coudert F-X. Necessary and sufficient elastic stability conditions in various crystal systems. *Phys Rev B*. 2014;90(22):224104.
51. Yang Y, Lu H, Yu C, Chen JM. First-principles calculations of mechanical properties of TiC and TiN. *J Alloys Compd*. 2009;485(1):542.
52. Shugani M, Chouhan SS, Aynyas M, Sanyal S. *Ab-initio* study of structural, electronic and elastic properties of ErCu. *Adv Phys Theor Appl*. 2013;19:83.
53. Chen K, Zhao LR. *Ab initio* study of elastic properties of Ir and Ir_3X compounds. *J Appl Phys*. 2003;93(5):2414.
54. Cherkaev A, Gibiansky L. Coupled estimates for the bulk and shear moduli of a two-dimensional isotropic elastic composite. *J Mech Phys Solid*. 1993;41(5):937.
55. Pettifor D. Theoretical predictions of structure and related properties of intermetallics. *Mater Sci Technol*. 1992;8(4):345.
56. Vaitheeswaran G, Kanchana V, Kumar RS, Cornelius A, Nicol M, Svane A, et al. High-pressure structural, elastic, and electronic properties of the scintillator host material $KMgF_3$. *Phys Rev B*. 2007;76(1):014107.
57. Murtaza G, Gupta S, Seddik T, Khenata R, Alahmed Z, Khachai H, et al. Structural, electronic, and thermodynamic properties of cubic $REGa_3$ (RE= Sc or Lu) compounds: *Ab initio* study. *J Alloys Compd*. 2014;597:36.
58. Rajagopalan M. Full potential linear augmented plane wave study of the elastic properties of XPt_3 (X= V, Cr, Mn, Fe, Co, Ni). *Phys B Condens Matter*. 2010;405(11):2516.
59. Mott P, Dorgan J, Roland C. The bulk modulus and Poisson's ratio of "incompressible" materials. *J Sound Vib*. 2008;312(4):572.
60. Tvergaard V, Hutchinson JW. Microcracking in ceramics induced by thermal expansion or elastic anisotropy. *J Am Ceram Soc*. 1988;71(3):157.
61. Greaves GN, Greer A, Lakes R, Rouxel T. Poisson's ratio and modern materials. *Nat Mater*. 2011;10(11):823.
62. Kleinman L. Deformation potentials in silicon. I. Uniaxial strain. *Phys Rev*. 1962;128(6):2614.
63. Ladwig PF, Chang YA, Linville ES, Morrone A, Gao J, Pant BB, et al. Paramagnetic to antiferromagnetic phase transformation in sputter deposited Pt–Mn thin films. *J Appl Phys*. 2003;94(2):979.
64. Anderson OL. A simplified method for calculating the Debye temperature from elastic constants. *J Phys Chem Solid*. 1963;24(7):909.
65. Pagare G, Chouhan SS, Soni P, Sanyal S, Rajagopalan M. Electronic, elastic and thermal properties of lutetium intermetallic compounds. *Solid State Sci*. 2013;18:141.